

The pVHL₁₇₂ isoform is not a tumor suppressor and up-regulates a subset of pro-tumorigenic genes including *TGFB1* and *MMP13*

Pauline Hascoet¹, Franck Chesnel¹, Florence Jouan^{1,**}, Cathy Le Goff¹, Anne Couturier¹, Eric Darrigrand², Fabrice Mahe², Nathalie Rioux-Leclercq³, Xavier Le Goff^{1,*} and Yannick Arlot-Bonnemains^{1,*}

¹CNRS, UMR 6290 IGDR, Université Rennes 1, BIOSIT, Rennes, France

²IRMAR, Université Rennes 1, Rennes, France

³CHU Rennes, Service d'Anatomo-Pathologie, Rennes, France

* Co-last authors

** Present address: INSERM U1242 –Université Rennes 1-Centre E Marquis Rennes, France

Correspondence to: Yannick Arlot-Bonnemains, **email:** yannick.arlot@univ-rennes1.fr
Xavier Le Goff, **email:** xavier.le-goff@univ-rennes1.fr

Keywords: von Hippel Lindau, tumor suppressor, human kidney cells, TGF- β signaling, metalloprotease

Received: February 14, 2017

Accepted: April 26, 2017

Published: June 06, 2017

Copyright: Hascoet et al. This is an open-access article distributed under the terms of the Creative Commons Attribution License 3.0 (CC BY 3.0), which permits unrestricted use, distribution, and reproduction in any medium, provided the original author and source are credited.

ABSTRACT

The von Hippel-Lindau (*VHL*) tumor suppressor gene is often deleted or mutated in ccRCC (clear cell renal cell carcinoma) producing a non-functional protein. The gene encodes two mRNA, and three protein isoforms (pVHL₂₁₃, pVHL₁₆₀ and pVHL₁₇₂). The pVHL protein is part of an E3 ligase complex involved in the ubiquitination and proteasomal degradation of different proteins, particularly hypoxia inducible factors (HIF) that drive the transcription of genes involved in the regulation of cell proliferation, angiogenesis or extracellular matrix remodelling. Other non-canonical (HIF-independent) pVHL functions have been described. A recent work reported the expression of the uncharacterized protein isoform pVHL₁₇₂ which is translated from the variant 2 by alternative splicing of the exon 2. This splice variant is sometimes enriched in the ccRCCs and the protein has been identified in the respective samples of ccRCCs and different renal cell lines. Functional studies on pVHL have only concerned the pVHL₂₁₃ and pVHL₁₆₀ isoforms, but no function was assigned to pVHL₁₇₂. Here we show that pVHL₁₇₂ stable expression in renal cancer cells does not regulate the level of HIF, exacerbates tumorigenicity when 786-O-pVHL₁₇₂ cells were xenografted in mice. The pVHL₁₇₂-induced tumors developed a sarcomatoid phenotype. Moreover, pVHL₁₇₂ expression was shown to up regulate a subset of pro-tumorigenic genes including *TGFB1*, *MMP1* and *MMP13*. In summary we identified that pVHL₁₇₂ is not a tumor suppressor. Furthermore our findings suggest an antagonistic function of this pVHL isoform in the HIF-independent aggressiveness of renal tumors compared to pVHL₂₁₃.

INTRODUCTION

The human von Hippel-Lindau (*VHL*) tumor suppressor gene encodes three different protein isoforms. The pVHL₂₁₃ (213 amino acids) and pVHL₁₆₀ (160 amino acids; absence of 54 NH₂-terminal amino acids due to the use of an internal start site) isoforms are translated from the full length mRNA [1, 2], whereas pVHL₁₇₂ (172 amino

acids) is encoded by an mRNA in which exon 2 is excluded by alternative splicing [3, 4]. *In vivo*, pVHL₂₁₃ and pVHL₁₆₀ exert equivalent functions. Specifically, they show tumor suppressor activity in a clear cell Renal Cell Carcinoma (ccRCC) cell xenograft model [2, 5]. The pVHL₂₁₃ is the substrate recognition subunit of an E3 ubiquitin ligase complex that also includes elongins B and C, cullin-2 and RBX1. This complex targets hypoxia-inducible factor

alpha (HIF- α) for proteasomal degradation. Inactivation of pVHL stabilizes HIF- α that heterodimerizes with HIF- β and translocates in the nucleus to activate the transcription of many genes involved in the hypoxic response and other pro-tumorigenic processes [6]. Loss of pVHL function is crucial in different pathologies and has been largely studied in ccRCC, the most common kidney cancer type. More than 80% of sporadic ccRCC show pVHL deficiency [4, 7]. Loss of *VHL* function by deletion, mutation or promoter hypermethylation contributes to ccRCC initiation by promoting HIF-dependent overproduction of proangiogenic factors, including VEGF and PDGF.

Moreover, other non-canonical (*i.e.*, HIF-independent) pVHL functions have been described, such as regulation of cell-cell interaction, matrix signaling and adhesion [8], which may also contribute to pVHL tumor suppressor activity [9]. For instance, extracellular fibronectin matrix is defective in renal carcinoma cells lacking pVHL, suggesting a direct pVHL role in fibronectin matrix formation. Loss of pVHL in ccRCC has also been associated with modulation of TGF β 1 expression and poor prognosis [10, 11]. Elevated levels of TGF β 1 in serum samples from patients with ccRCC are correlated with unfavorable outcome and ccRCC microenvironment is TGF β 1-rich. TGF β binding to and activation of the TGF β receptors TGFBR1 and TGFBR2 at the plasma membrane activates the TGF β signaling pathway. Activated TGFBR1 phosphorylates SMAD2 and/or SMAD3 that form a complex with SMAD4 to regulate transcription of many target genes [12].

The pVHL₁₇₂ isoform was recently differentially detected in cells and tumor tissues and its putative effect on tumor progression needs to be investigated. Importantly, it has been reported that some *VHL* mutations may favor the expression of VHL variant 2 in ccRCC [4, 13, 14]. To determine how this pVHL₁₇₂ enrichment in some tumoral cell may affect tumor development, we stably expressed pVHL₁₇₂ in 786-O cells (derived from a human primary clear cell renal adenocarcinoma: pVHL null cells). Mice xenografted with pVHL₁₇₂-expressing 786-O cells developed tumors with more extended sarcomatoid phenotype than tumors derived from parental 786-O cells. Expression of pVHL₁₇₂ stimulated TGF β signaling and upregulation of the metalloproteases MMP13 and MMP1, while pVHL₂₁₃ expression downregulated these genes. Our study unravels a pVHL₁₇₂ positive role in tumor progression, suggesting that the expression balance of the different pVHL isoforms has a critical role in ccRCC initiation and progression.

RESULTS

The expression of pVHL₁₇₂ modifies behavior of 786-O cells

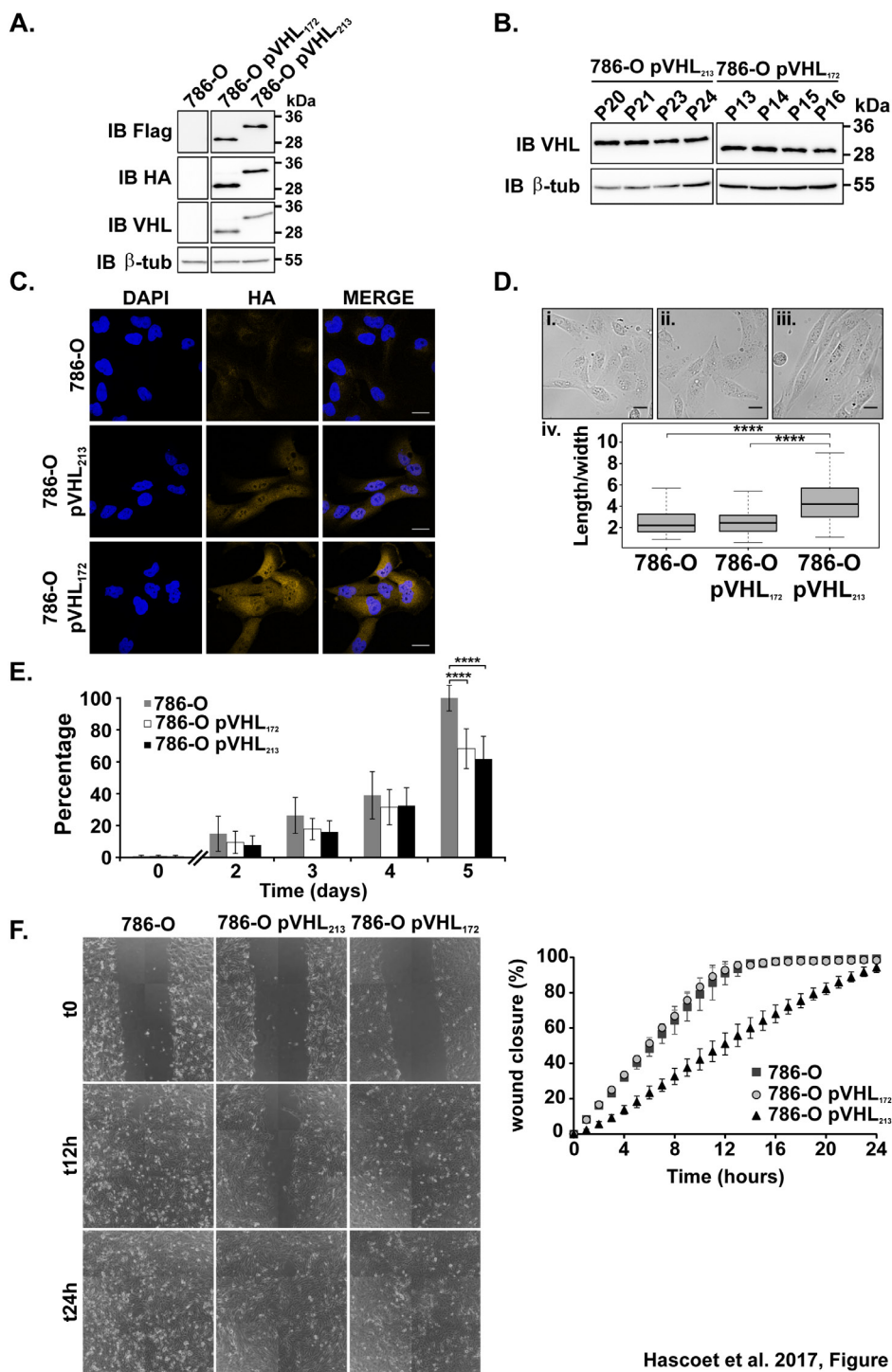
The *vhl* gene encodes two mRNA variants and three different protein isoforms (Supplementary Figure 1).

The expression of the variant 2 mRNA of the *vhl* gene was evidenced and the presence of the corresponding protein was detected in different cells lines and in renal tumor tissues [3]. Whereas pVHL₂₁₃ was characterized as a tumor suppressor gene, pVHL₁₇₂ function has never been investigated yet. In order to investigate this pVHL₁₇₂ function we generated stably transfected cells lines with pVHL₁₇₂ (or pVHL₂₁₃ as a control). The level of pVHL expression was stable over several passages in both cell line (Figure 1A, 1B). Analysis of the half-life of the proteins showed a slight decrease in pVHL₂₁₃ expression after 6 hours of incubation with cycloheximide (CHX, Supplementary Figure 2A). Conversely, pVHL₁₇₂ expression remained stable, whereas cyclin D (CCD1) expression (used as positive control) strongly decreased after 30 min of CHX incubation, in agreement with published results [15]. Anti-HA immunostaining showed that pVHL was broadly expressed in all cells in pVHL₁₇₂-expressing and pVHL₂₁₃-expressing 786-O cells, but not in parental 786-O cells (Figure 1C). pVHL₁₇₂ expressing 786-O cells are more spread than the pVHL₂₁₃-expressing 786-O cells (Figure 1D) as confirmed by tubulin network labelling (Supplementary Figure 2B). The cell width and length were measured in the three cell lines (n=100 cells). The length/width ratio of 786-O and 786-O-pVHL₁₇₂ cells was comparable (2.7 and 2.6, respectively) (Figure 1D.i and 1D.ii), whereas it was significantly higher in 786-O-pVHL₂₁₃ cells (4.6) (Figure 1D iii. and 1D iv.).

We then performed functional assays to determine whether the expression of pVHL₁₇₂ modified cell behavior compared to the cells expressing pVHL₂₁₃. The cell proliferation was significantly slowed down (at day 5) in cells that expressed pVHL₁₇₂ or pVHL₂₁₃ compared with parental 786-O cells (no pVHL expression) ($p = 1.24 \times 10^{-13}$ and, $p = 4.341 \times 10^{-13}$ respectively) (Figure 1E). Analysis of cell motility by using a wound-healing assay showed complete closure of the wound after 12 hours in 786-O and 786-O-pVHL₁₇₂ cells. Conversely, wound closure was not complete in 786-O-pVHL₂₁₃ cells even after 24 hours (Figure 1F). This was caused by cell migration inhibition and not the result of both cell migration and proliferation defects because identical results were obtained in the presence of mitomycin C to inhibit cell proliferation (Supplementary Figure 2C). The expression of pVHL₁₇₂ conferred to the 786-O cells behavior modifications related occasionally to the 786-O-pVHL₂₁₃ cells or to the 786-O and this prompted us to consider the tumor suppressor gene function of this isoform *in vivo*.

The expression of pVHL₁₇₂ induces an oncogenic phenotype in 786-O cells and does not act as a tumor suppressor in mice

A 3D *in vitro* cell culture model assay was adopted as a preclinical model tool for studying tumor cell behaviour.



Hascoet et al. 2017, Figure 1

Figure 1: Analysis of the phenotypes of the cells expressing pVHL₁₇₂ or pVHL₂₁₃. (A) pVHL expression in 786-O, 786-O-pVHL₁₇₂ and 786-O-pVHL₂₁₃ cells assessed by immunoblotting with the indicated antibodies. (B) pVHL expression at different passages in the stable 786-O-pVHL₁₇₂ and 786-O-pVHL₂₁₃ cell lines assessed by immunoblotting. (C) pVHL expression analyzed by immunocytochemistry with an anti-HA antibody in 786-O (upper panels), 786-O-pVHL₂₁₃ (middle panels) and 786-O-pVHL₁₇₂ cells (lower panels). Nuclei were stained with DAPI (scale bar: 25 μm). (D) The length and width of 786-O cells (i), 786-O-pVHL₁₇₂ (ii) and 786-O-pVHL₂₁₃ (iii) cells were measured and the length/width ratio (iv) was calculated (n=100/each, ****: p<0.0001, Mann-Whitney test). Scale bar: 25 μm. (E) Proliferation of 786-O, 786-O-pVHL₁₇₂ and 786-O-pVHL₂₁₃ cells was assessed using the PrestoBlue™ assay. Values were normalized to the mean 786-O cell number at day 5 (mean±s.d. of three independent experiments with eight independent samples; ****: p<0.0001, Mann-Whitney test performed at day 5). (F) Analysis of cell migration by wound healing assay. Results were expressed as the percentage of wound closure at the indicated time points (mean±s.d. of three independent samples representative of three independent experiments).

A spheroid formation assay was made to determine whether pVHL₁₇₂ expression in cells could modify the properties of the 786-O cells to aggregate. Cultivating the cells on a non-adherent surface induced the formation of spheroids in the case of 786-O cells (mean size 0.12 mm², n=58) and the 786-O-pVHL₁₇₂ cells (mean size 0.16 mm², n=45) (Figure 2A). In contrast, the 786-O-pVHL₂₁₃ cells did only form cell clumps. Interestingly, the expression of pVHL₁₇₂ in cells induced spheroids formation which size was significantly larger (Figure 2A, right panel; p-value=3.805 10⁻⁵). This assay demonstrated that the expression of pVHL₁₇₂ did not suppress cell aggregation as observed with the expression of pVHL₂₁₃. In order to further explore this property, we used a heterotopic cell line derived xenograft model. Ten millions of 786-O, 786-O-pVHL₂₁₃ or 786-O-pVHL₁₇₂ cells were injected subcutaneously in nude mice. The injection of 786-O-pVHL₂₁₃ cells failed to induce tumor in mice (n=8) after 16 weeks. The volume of each tumor growing from 786-O or 786-O-pVHL₁₇₂ cells was monitored twice a week (Supplementary Table 1). The tumors (75 mm³) were detectable after three and seven weeks for 786-O cells and 786-O pVHL₁₇₂ cells, respectively. The size of the tumors increased up to the end of the experiment (Figure 2B). We found no evidence of metastases formation. We fitted the experimental values of individual growth for each tumor using a second degree polynomial interpolation. The average “start” value (defining when the tumor was measurable) was 3.64±0.97 weeks for 786-O tumors and 4.42±0.65 weeks for 786-O-pVHL₁₇₂ tumors, suggesting a delayed growth induction for 786-O-pVHL₁₇₂ cell-derived tumors but that was statistically non significant. During the effective tumor growth, the asymptotic speed of growth of 786-O-pVHL₁₇₂ tumors was significantly higher (4.20±0.78 vs 3.12±0.65 for 786-O tumors; t-test : p=0.044). When analysing later time points from weeks 5 to 10, the growth rate of 786-O-pVHL₁₇₂ tumors was higher than that of 786-O tumors (860 mm³ and 551 mm³ at 10.5 weeks for 786-O-pVHL₁₇₂ and 786-O respectively). Expression of the pVHL₁₇₂ performed on the harvested 786-O-pVHL₁₇₂ cell-derived tumors revealed the presence of pVHL over time, (Figure 2C). Thus pVHL₁₇₂ expression slightly delayed tumor growth induction, but then increased tumor growth speed. This result indicated that opposite to the long pVHL₂₁₃ isoform, pVHL₁₇₂ expression in kidney cancer cells did not exert a tumor suppressor function but rather induces dissimilar morphological modifications in spheroids as in tumor compared to the spheroids or tumors generated with the parental 786-O cells.

The striking and consistent differences in the morphology between spheroids and tumors expressing pVHL172 prompted us to examine the molecular a biochemical parameters in the structures. A hallmark of renal tumors is the sarcomatoid changes considered as terminally dedifferentiated status. We performed

hematoxylin and eosin (HE) staining on sections of 786-O and 786-O-pVHL₁₇₂ tumors and spheroids (Figure 2D, Supplementary Figure 3). We observed cells with large and clear cytoplasm in the non sarcomatoid regions while the sarcomatoid phenotype was characterised by the presence of elongated, spindle-shaped, cells (Figure 2D). Interestingly, the sarcomatoid component was significantly higher in 786-O-pVHL₁₇₂ derived tumors as it represented 99.1±1.5% in those tumor sections vs 78.6±17.3% in 786-O cell-derived tumor sections (p<0.05) (Figure 2D). An identical observation was made with HE-stained spheroids (Supplementary Figure 3). Delimitation and measurement of necrotic areas in HE-stained tumor sections did not highlight more than 5% of necrotic areas in 786-O-pVHL₁₇₂ tumors (data not shown). In summary to these observations, we concluded that the expression of pVHL₁₇₂ rather promoted a higher percentage of the sarcomatoid phenotype in tumors that is correlated to a poor prognostic factor in kidney cancer. Collectively, all the results indicated that expression of pVHL₁₇₂ exacerbates molecular pathways previously observed in tumoral VHL null cells (*i.e.* 786-O parental cells).

pVHL₁₇₂ expression in cells induces specific metalloproteases over-expression

Proteolytic degradation of the extracellular matrix is considered as essential step for invasion and metastasis by cancer cells and malignant transformation has been often shown to associate with alteration of several metalloproteases [16]. MMP expression and activity in the three cell lines were assessed with two different zymography assays (Figure 3A).

The gelatinase assay in non-reducing conditions was originally used to check MMP2 and MMP9 activity levels. Extracts from 786-O cells induced digestion areas at ~95, ~80 and ~65 kDa that corresponded to the molecular weights of pro-MMP2/MMP2 and pro-MMP9/MMP9, respectively (Figure 3A). A digestion area at the pro-MMP2 level was observed with 786-O-pVHL₁₇₂ cell extracts, whereas no or modest degradation was observed with 786-O-pVHL₂₁₃ or 786-O cell extracts. Moreover, a stronger degradation area at around ~45 kDa was detected in 786-O-pVHL₁₇₂ and 786-O cell extracts (to a lesser extent) (Figure 3A, low MW MMP). These results suggest that pVHL₁₇₂ expression may promote the expression and/or activity of low MW MMPs, which include MMP1, -3, -8, -13 or -23. A second zymography assay with collagen type I as substrate has confirmed this result (data not shown). As MMP1, MMP8 and MMP13 are all known as both gelatinases and collagenases (collagen I), we investigated whether these MMPs may be target of pVHL₁₇₂ expression. Among all selected MMPs, a q-PCR analysis using RNA extracted from the three cell lines showed that only *MMP1* and *MMP13* mRNAs were upregulated in 786-O-pVHL₁₇₂ cells compared with 786-

O and both were down-regulated in 786-O-pVHL₂₁₃ cells. The MMP2 expression was not significantly changed in the three cell lines (Figure 3B). No difference in *MMP9* mRNA expression could be detected in any of the three cell lines (data not shown). The immunohistochemistry analysis of MMP13 expression in tumors derived from 786-O-pVHL₁₇₂ cells and parental 786-O cells (control) showed a stronger MMP13 signal in pVHL₁₇₂-expressing tumors than in controls (Figure 3C). None of the tumor

expressing pVHL₁₇₂ showed an increased signal for MMP1. Thus we focused our analysis on MMP13. To confirm that *MMP13* upregulation was pVHL₁₇₂-dependent, pVHL₁₇₂ was knocked down in 786-O-pVHL₁₇₂ cells by using a specific VHL₁₇₂ siRNA (SiVHL). Upon SiVHL transfection, pVHL₁₇₂ expression was reduced by 82% compared with non-transfected cells and cells transfected with control siRNA (SiC) (Figure 3D). The amount of MMP13 mRNA did not change between 786-

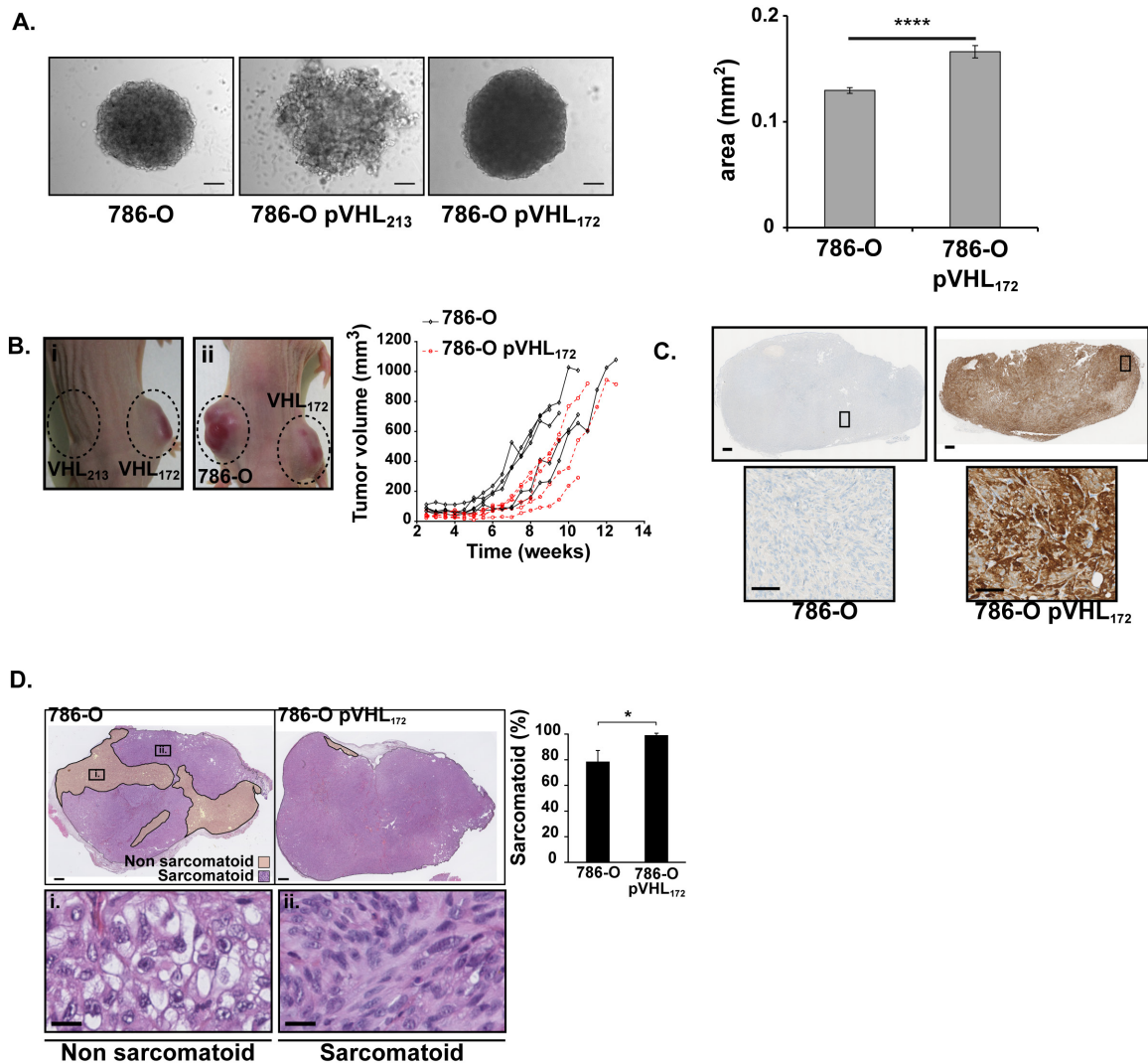


Figure 2: Tumorigenic effect 786-O-pVHL₁₇₂ cell-derived tumors compared with 786-O cell-derived tumors. (A) Morphology of 786-O, 786-O-pVHL₂₁₃ and 786-O pVHL₁₇₂ spheroids (left panels). Spheroid areas from 786-O and 786-O-pVHL₁₇₂ cells were measured with the ImageJ software (right histogram, mean±sem, n=58 and n=45 respectively; Mann-Whitney test, ****: p<0.0001). Scale bars: 100 μm. **(B)** External morphology of tumors obtained by xenografting 786-O-pVHL₁₇₂ de mice (i-left flank and ii-right flank), 786-O-pVHL₂₁₃ (i-right flank) or 786-O cells (ii-left flank) in nude mice. Growth kinetics of 786-O and 786-O-pVHL₁₇₂ derived tumors determined by measuring the tumor volumes using a caliper (n=5 tumors per cell type). **(C)** pVHL₁₇₂ expression was controlled by immunohistochemical staining with an anti-HA antibody in 786-O-pVHL₁₇₂ and 786-O cell-derived tumors (upper panels; scale bar: 500μm). A 20X magnification is shown in the lower panels (scale bar: 100μm). **(D)** Sarcomatoid and non-sarcomatoid areas were delimited following HE staining of 786-O and 786-O-pVHL₁₇₂ cell-derived tumor sections (upper panels, scale bar: 500μm). Inserts in a representative 786-O tumor section show the gradual progression of the tumor phenotype from (i) non-sarcomatoid morphology to (ii) a tissue with sarcomatoid component (scale bar: 20μm). The histogram shows the percentage of sarcomatoid areas relative to the whole tumor section (mean ± s.d., n=5 tumors/cell type; Mann-Whitney test: p<0.05).

O and control SiRNA transfected cells. In contrast, the relative amount of *MMP13* mRNA was significantly reduced in pVHL₁₇₂-depleted cells (Figure 3E), indicating that *MMP13* expression may be regulated by the expression of pVHL₁₇₂. Altogether, these results show that conversely to pVHL₂₁₃, pVHL₁₇₂ upregulates directly or indirectly the collagenase MMP13.

pVHL₁₇₂ does not down-regulate HIF-2 α expression even if it still participates to the E3 ubiquitin ligase complex

In recent years, our understanding of pVHL function has broadened to include several HIF-independent features. Hypoxia and HIFs can induce tumor

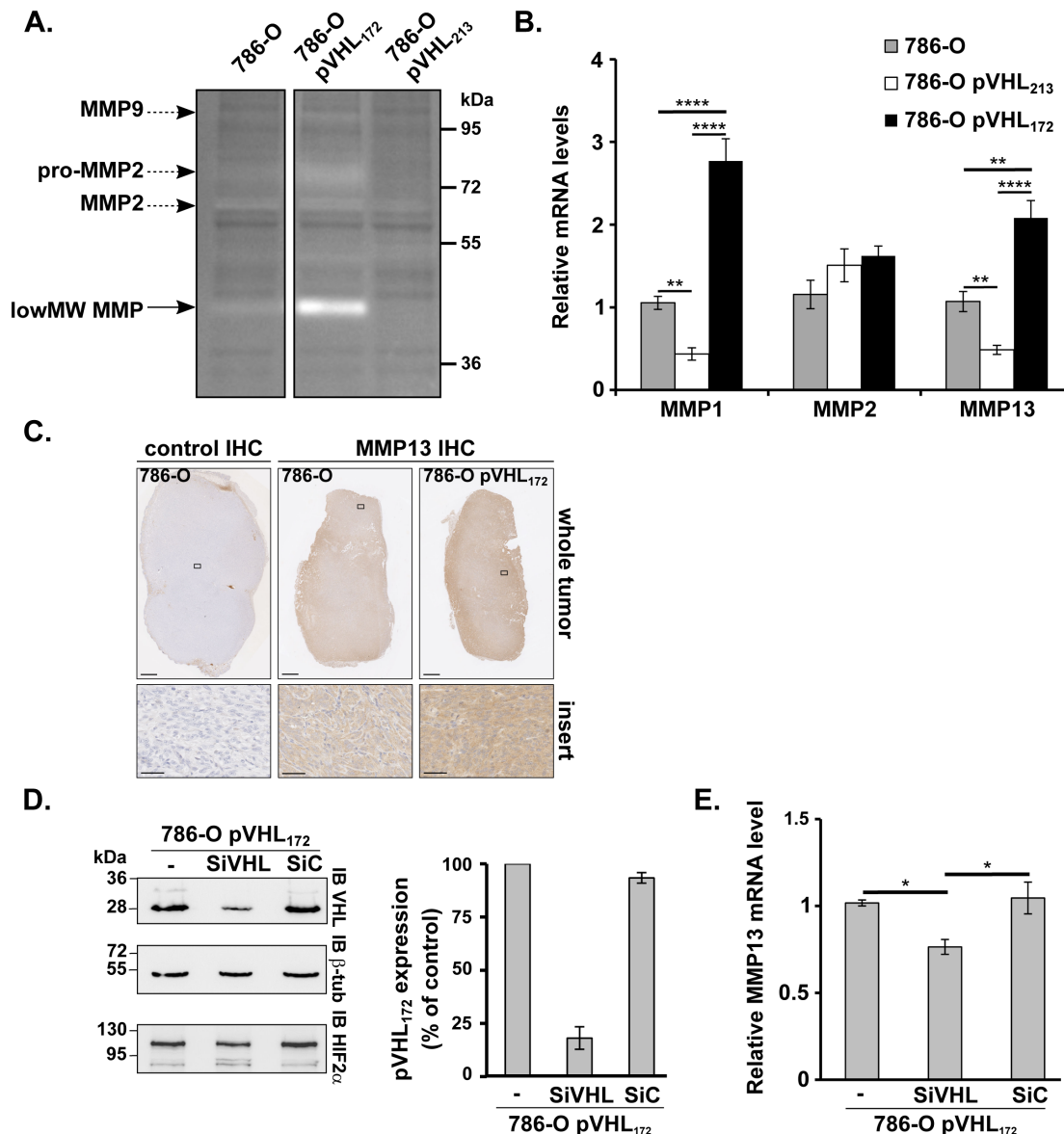


Figure 3: pVHL₁₇₂ promotes *MMP13* upregulation. (A) Zymography assay performed using gelatin-containing gels and 786-O, 786-O-pVHL₁₇₂ and 786-O-pVHL₂₁₃ protein extracts. Arrows indicate the digestion areas corresponding to the different pro-MMPs or MMPs, according to their molecular weights. Low MW MMP: low molecular weight MMPs (possibly MMP1, -3, -8, -13, or -23). (B) RT-qPCR assays using reverse-transcribed RNAs extracted from 786-O, 786-O-pVHL₂₁₃ and 786-O-pVHL₁₇₂ cells were performed to monitor the expression of *MMP1*, *MMP2* and *MMP13*. (C) *MMP13* expression analyzed by immunohistochemistry in whole 786-O and 786-O-pVHL₁₇₂ cell-derived tumors (upper panels; scale bar: 1 mm). A 40X magnification is shown in the lower panels (scale bar: 50 μ m). Control: secondary antibody alone (left panels). (D) Efficiency of siRNA-mediated pVHL₁₇₂ downregulation assessed by immunoblotting with anti-pVHL₁₇₂ and β -tubulin (control) antibodies in 786-O-pVHL₁₇₂ cells harvested 72 hours after transfection with siRNAs against *VHL* RNA variant 2 (SiVHL), control siRNA (SiC) or transfection reagent alone (-). The histogram shows the quantification of the results (mean \pm SEM; n=4); pVHL₁₇₂ expression in control cells (-) was set to 100. (E) RT-qPCR analysis of *MMP13* expression in 786-O-pVHL₁₇₂ cells transfected with SiVHL, SiC or transfection reagent alone (-). RNA levels were normalized to *GAPDH* and *RPLPO* and the expression level in control 786-O-pVHL₁₇₂ cells (-) was set to 1. (n=4). *: p < 0.05; **: p < 0.01; ***: p < 0.001; ****: p < 0.0001, Mann-Whitney test.

cell invasion and degradation of the extracellular matrix *via* various mechanisms including upregulation of matrix metalloproteinases-1 and -2 [17, 18]. In chondrocytes, HIF-2 α directly induces the expression of genes encoding catabolic factors, including matrix metalloproteinases (*MMP1*, *MMP9*, *MMP12* and *MMP13*) [19]. We wonder whether pVHL₁₇₂ might regulate the expression of the MMPs in a HIF-dependent way. HIF amount in cells is regulated by the E3 ligase complex in which pVHL protein assembles with associated proteins: elongins B and C, cullin-2, and Rbx. This E3 ubiquitin ligase targets the α -subunits of hypoxia-inducible factor (HIF α) for oxygen-dependent degradation. HIF-2 α is stabilized by hypoxia or mutations of pVHL. In pVHL₂₁₃, exon 2-encoded residues 114–154 are mostly hydrophobic and are hypothesized to play a role in substrate protein recognition, although *in vitro* experiments have revealed that they might not be required for pVHL binding to HIF α [20]. In order to understand the absence of tumor suppressor function for pVHL₁₇₂, we investigated whether HIF-2 α is regulated by this isoform by first studying the belonging of pVHL₁₇₂ to the same E3 ligase complex. Total protein extracts from 786-O-pVHL₁₇₂, 786-O-pVHL₂₁₃ and parental 786-O cells were analysed by immuno-precipitation assay (Figure 4A). Elongin C and cullin-2 co-immunoprecipitated with Flag-tagged pVHL₂₁₃, as expected, and also with Flag-tagged pVHL₁₇₂ (Figure 4A). Conversely, none of these proteins were found in the fraction immunoprecipitated from 786-O cells (Figure 4A). We secondly confirmed that the protein HIF-2 α was not degraded in cells expressing pVHL₁₇₂ compared to the 786-O-pVHL₂₁₃ cells and was similar to that of the parental 786-O cell line under normoxia or hypoxia conditions (Figure 4B). Likewise, HIF-2 α was not degraded in spheroids resulting from 786-O expressing or not pVHL₁₇₂; it was even notably higher in spheroids expressing pVHL₁₇₂ compared to the 786-O-derived spheroids (Figure 4C-4D). These results highlighted that pVHL₁₇₂ does not regulate HIF stability but still retain the capacity to form a E3 ubiquitin ligase complex. As the 786-O and the 786-O-pVHL₁₇₂ shared the same HIF-2 α status, we speculated that exacerbation of tumorigenic features in cell lines which expressed pVHL₁₇₂ may therefore be regulated by alternative HIF-independent pathway(s).

pVHL₁₇₂ regulates the expression of MMPs via the TGFB signalling

The cytokine Transforming Growth Factor- β (TGF- β) has been extensively studied in tumor biology and is believed to serve a variety of functions in tumor progression. Increased expression of the MMPs (MMP13 in particular) was also demonstrated to be stimulated by TGFB1 [21]. We analysed the *TGFB1* mRNA by RT-qPCR and observed a significant increase in 786-O-pVHL₁₇₂ cells compared with parental 786-O cells

(Figure 5A). To determine whether this increase was accompanied by *TGFB* signalling activation, total SMAD3 and phosphorylated SMAD3 (pSMAD3) levels were assessed by western blotting. Compared with parental 786-O cells, pSMAD3 was significantly increased in 786-O-pVHL₁₇₂ cells and reduced in 786-O-pVHL₂₁₃ cells (Figure 5B). Moreover, a 24-hour incubation with SB431542, a TGFB1 inhibitor, did not affect *TGFB1* mRNA up regulation (Figure 5C) but markedly reduced pSMAD3 level in 786-O-pVHL₁₇₂ cells (Figure 5D). As pVHL₁₇₂ was suspected to control the MMPs levels via the TGFB signalling, the effect of this TGFB1 inhibitor on *MMP13* expression in 786-O-pVHL₁₇₂ cells was assessed by RT-qPCR analysis. The experiment showed that TGFB signalling inhibition reduced the expression of *MMP13* (Figure 5E). Conversely, when incubating the 786-O cells in the presence of TGFB, we observed a two-fold increase of *MMP13* expression (Figure 5F). Having demonstrated that pVHL₁₇₂ induced the expression of *MMP13* in cells in a TGFB-dependent manner, we further tested the expression of both *MMP13* and TGFB *in vitro* in the 3D spheroid models. In spheroids expressing pVHL₁₇₂, we first observed an increase of TGFB mRNA (Figure 5G) associated with an increase of *MMP13* transcript expression (Figure 5H). These findings clearly demonstrate the ability of pVHL₁₇₂ to positively regulate *MMP-13* expression via TGFB signaling in 786-O-pVHL₁₇₂ cells and suggest that Smad/pSmad may participate in this (TGFB) regulatory pathway.

DISCUSSION

In this work, we show that contrarily to the long isoform pVHL₂₁₃, pVHL₁₇₂ is not a tumor suppressor but rather exacerbates renal tumor phenotype. Specifically, we demonstrated in our model that: (a) pVHL₁₇₂ expression in 786-O cells does not modify the cell phenotype, but reduces cell proliferation, (b) cultured on non-adherent surface, pVHL₁₇₂-expressing cells generates larger spheroids (c) when xenografted in mice, pVHL₁₇₂-expressing 786-O cells produce tumors with a higher sarcomatoid component compared with tumors derived from parental cells (d) the function of pVHL₁₇₂ does not depend upon HIF-2 α regulation. Our results strongly suggest that the tumor phenotype could be in part dependent on pVHL₁₇₂-mediated upregulation of *TGFB1* and of some metalloproteases.

Loss of the *VHL* gene plays an important role in the development of sporadic or hereditary ccRCC in some patients with *VHL* disease [4]. Here, we show that in contrast to pVHL₂₁₃, expression of pVHL₁₇₂ in 786-O cells does not inhibit tumor growth and promotes a more dedifferentiated tumoral phenotype compared to the tumors induced with parental 786-O cells.

Literature data indicate that pVHL is involved in the fine regulation of cell proliferation, survival and

angiogenesis by controlling the stability of hypoxia inducible transcription factors α (HIF-1 α , HIF-2 α and HIF-3 α , collectively HIF- α) [22]. pVHL interact with elongin C (*via* their α domain), elongin B and cullin-2 in an E3 ubiquitin ligase complex that targets substrates for

degradation by the proteasome. Interestingly, like pVHL₂₁₃, pVHL₁₇₂ also can interact in the E3 ligase complex by association with elongins B & C and cullin-2. However, it does not have any effect on HIF stability in normoxic conditions (Figure 4). Moreover, overexpressed pVHL₁₇₂

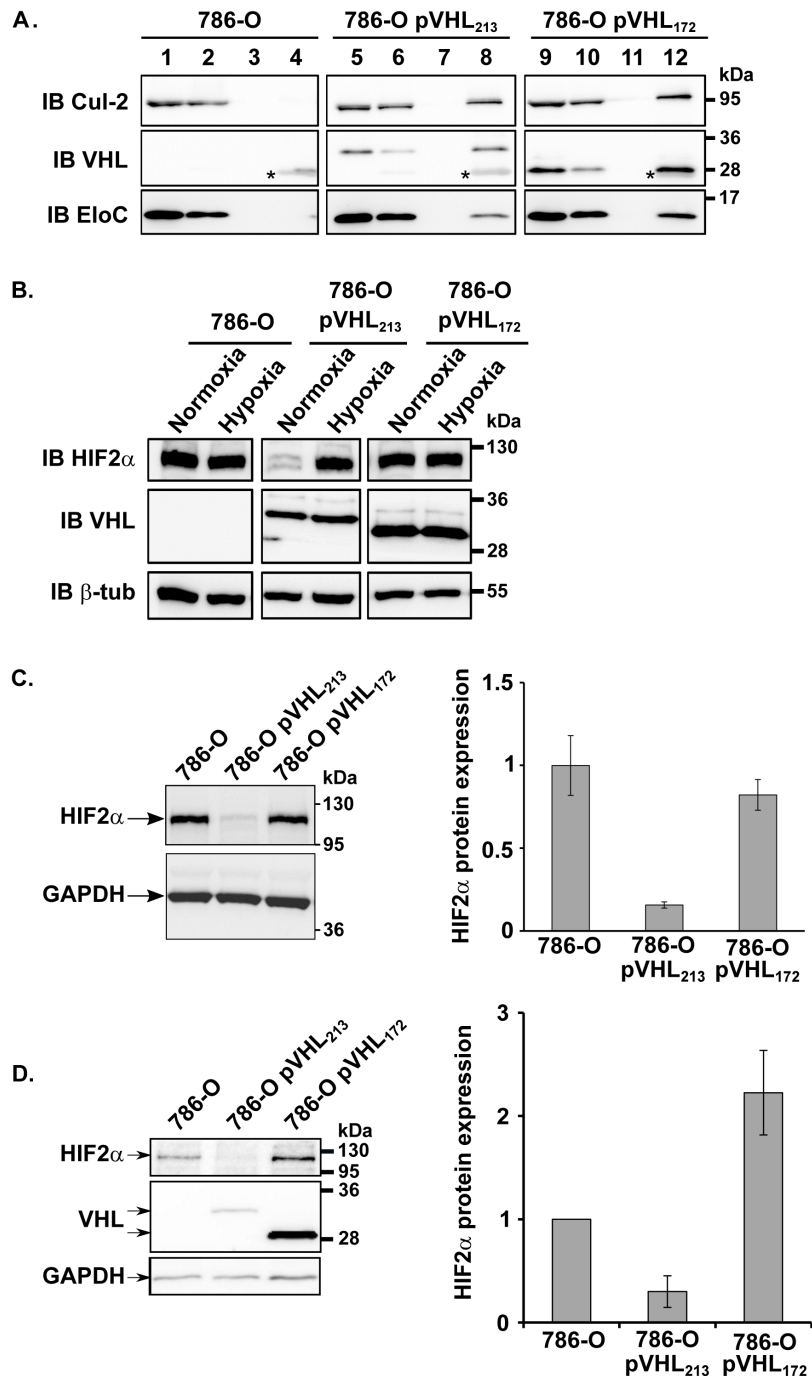


Figure 4: pVHL₁₇₂ is part of an E3 ubiquitin ligase complex, but is not involved in HIF-2 α down-regulation. (A) pVHL, cullin-2 and elongin C expression in cell lysates (1, 5, 9), unbound (2, 6, 10), wash (3, 7, 11) and Flag-immunoprecipitated (4, 8, 12) fractions of 786-O, 786-O-pVHL₂₁₃ and 786-O-pVHL₁₇₂ cells was assessed by immunoblotting (*: IgG light chain). (B) HIF-2 α protein expression level was evaluated by immunoblotting in 786-O, 786-O-pVHL₂₁₃ and 786-O-pVHL₁₇₂ cells in normoxia or hypoxia conditions. β -Tubulin was used as a loading control to quantify the level of HIF-2 α . (C-D) HIF-2 α expression level was evaluated by immunoblotting in 786-O, 786-O-pVHL₂₁₃ and 786-O-pVHL₁₇₂ spheroids. GAPDH was used as a loading control to quantify the level of HIF-2 α .

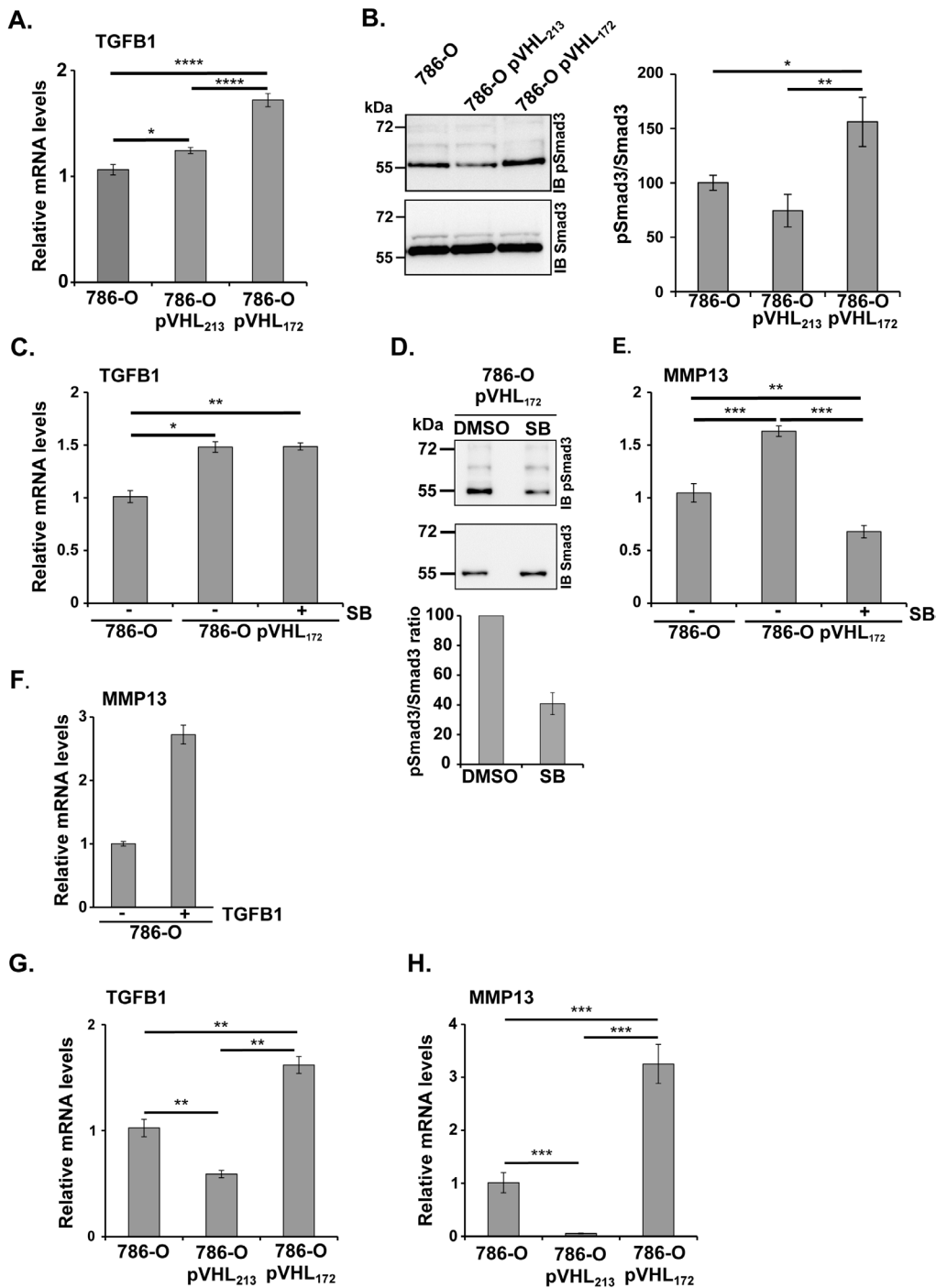


Figure 5: pVHL₁₇₂ promotes TGFB and MMP13 upregulation. (A) RT-qPCR analysis of *TGFB* expression in 786-O, 786-O-pVHL₁₇₂ and 786-O-pVHL₂₁₃ cells. *GADPH* was used as control. (*: p<0.05; ****: p<0.0001; ANOVA test). (B) Phosphorylated SMAD3 (upper panel) and total SMAD3 levels (lower panel) in 786-O, 786-O-pVHL₁₇₂ and 786-O-pVHL₂₁₃ cells were assessed by western blot analysis. Histogram on the right shows the quantification of the phosphorylated SMAD3/total SMAD3 ratio in 786-O, 786-O-pVHL₂₁₃ and 786-O-pVHL₁₇₂ cells. (*: p<0.05; **: p<0.01; ANOVA test). (C) RT-qPCR analysis of *TGFB* mRNA expression in 786-O and 786-O-pVHL₁₇₂ cells incubated with SB431542 (SB) or with DMSO (control). Control *TGFB* mRNA levels (DMSO-treated 786-O cells) was set to 1. (D) Phosphorylated SMAD3 (upper panel) and total SMAD3 (lower panel) level was assessed by immunoblotting in 786-O-pVHL₁₇₂ cells treated with SB431542 (SB), a TGFB receptor inhibitor, or with DMSO. The phosphorylated SMAD3/total SMAD3 ratios are shown in the histogram; the ratio of control cells (DMSO) was set to 100. (E) RT-qPCR analysis of *MMP13* mRNA expression in 786-O and 786-O-pVHL₁₇₂ cells incubated with SB431542 (SB) or with DMSO (control). Control mRNA levels (DMSO-treated 786-O cells) was set to 1. (F) RT-qPCR analysis of *MMP13* expression in 786-O cells incubated with the TGFB (5 ng/ml). (**: p<0.01; ***: p<0.001; Mann-Whitney test). (G-H) Rt-qPCR analysis of *TGFB* (G) and *MMP13* (H) expression in spheroids of 786-O, 786-O-pVHL₁₇₂ and 786-O-pVHL₂₁₃ cells. (**: p<0.01; ***: p<0.001; Mann-Whitney test).

does not compete with pVHL₂₁₃ for the binding to other E3 ligase components and consequently, does not antagonize pVHL₂₁₃-mediated HIF regulation (Supplementary Figure 4). This suggests that pVHL₁₇₂, as part of the cullin-2/elongin B/elongin C/RBX1 complex, could act as a new E3 ligase substrate recognition component, unrelated to hypoxia signaling. The absence of part of the VHL β domain in pVHL₁₇₂ might alter the sheet number and position in the structure and this could modify some protein functional activities such as specificity of substrate recognition.

We demonstrated that the pVHL₁₇₂ isoform has an opposite effect on renal tumor progression compared with full-length pVHL₂₁₃. pVHL₂₁₃-expressing tumor cells show reduced cell proliferation, motility and invasion *in vitro* [23]. In contrast, motility and invasiveness of pVHL₁₇₂-expressing cells and parental 786-O cells are undistinguishable. Only cell proliferation was slower in 786-O-pVHL₁₇₂ cells, possibly explaining the slightly slower initial growth of tumors derived from 786-O pVHL₁₇₂ cells compared with 786-O cells.

Our study also evidences that pVHL₁₇₂ expression correlates with a higher proportion of sarcomatoid areas in tumor sections. We also observe an immature vasculature in the tumors expressing pVHL₁₇₂ (Supplementary Figure 5). As previously mentioned, tumor vessels remain immature and lack the tight association between mural cells and endothelial tubes dependent on the excessive VEGF synthesis [24, 25]. Moreover, sarcomatoid differentiation usually arises within high-grade ccRCC representing a late step in the progression of this tumor type [26]. This phenotype could result from HIF-mediated transcriptional activation of VEGF and many other pro-angiogenic genes in a severe hypoxic environment [27]. However, besides HIF-2α stabilization in pVHL₁₇₂-expressing cells, impaired angiogenesis due to overexpression of MMP1 and MMP13, which have been implicated in vascular regression [18], could also contribute to the increase in immature vasculature. Other mechanisms cannot be excluded. Several lines of evidences suggest that the function of VHL is likely to extend beyond its crucial role in oxygen signal transduction, and the loss of its function may result in deregulation of several signalling pathways that play key roles in biological processes such as cell proliferation, cell survival, cell invasion and metastasis [28].

High percentage of sarcomatoid transformation has been associated with worse outcome in patients with ccRCC [29]. The sarcomatoid component of RCC has been correlated with TGFB pathway activity [30, 31]. TGFB is upregulated in renal carcinoma and its overexpression is associated with Fuhrman grade III and IV cancers and the presence of metastases [32, 33]. Here, we found that in pVHL₁₇₂-expressing cells, TGFB1 is upregulated and this could also promote cell invasiveness. Conversely, pVHL₂₁₃ negatively regulates TGFB expression at both the transcriptional and protein levels [10]. Among the different

targets of TGFB signaling, SMAD- and MAPK-dependent upregulation of the matrix metalloproteinase MMP13 has been reported [34]. Moreover, different MMPs are upregulated in ccRCC and their expression correlates with advanced tumor grades, reduced cell survival and the presence of metastases [35, 36]. Particularly elevated levels of MMP2 and MMP9 were found in various cancers as kidney and are associated to a poor prognosis [37]. Recently, Sassano *et al.* also reported that high MMP-13 expression correlated significantly with adverse overall survival, while MMP-1 independently did not show any significant correlation with survival [38]. Moreover, MMP13 level has been shown to be regulated by TGFB induced signals [39].

Here, we show that the TGFB pathway downstream effector SMAD3 is consistently more phosphorylated in pVHL₁₇₂ expressing cells, indicating hyper activation of the TGFB canonical pathway associated with an overexpression of *MMP13* and *MMP1* genes. Incubation of 786-O-pVHL₁₇₂ cells with an inhibitor of TGFB signalling shows that the expression of *MMP13* is controlled by pVHL₁₇₂ through TGFB-dependent mechanisms. Consistently, *MMP13* expression was also increased in 786-O-pVHL₁₇₂ cell-derived spheroids and tumors compared with 786-O cell-derived spheroids and tumors. The molecular mechanisms by which pVHL₁₇₂ regulates TGFB and MMPs expression appear to be HIF-2α independent. Previous proteomic analysis reported SETDB1 and TCF25 as interactors for pVHL (Δ114-154) [40]. These proteins were recognized as co transcriptional repressor for respectively Runx2 and SRF, both involved in the transcriptional co-regulation for genes like MMP13 or MMP1 [41, 42]. We made the hypothesis that in these two cases, pVHL₁₇₂ by interacting with SETDB1 or TCF25, could interfere with their inhibitory effect on Runx2 or SRF. The precise cellular mechanisms by which pVHL₁₇₂ regulates TGFB and MMPs expression remain however to be clarified.

In conclusion, the von Hippel Lindau isoform pVHL₁₇₂ is not a tumor suppressor protein. Moreover, it does not simply behave as a dominant negative form of pVHL₂₁₃ as its expression in 786-O cells triggers the formation of higher sarcomatoid xenograft tumors compared with parental 786-O cells that do not express pVHL. Our findings suggest a critical role of pVHL₁₇₂ in activating a subset of pro-tumorigenic genes, including *TGFB* and *MMP13*. Future work will be focused on characterization of the mechanistic links between pVHL₁₇₂ HIF-independent functions *via* TGFB and/or the E3-ligase complex in cancer cell invasion and metastasis formation to consider new therapeutic strategies in the ccRCC. Our data support that the presence of pVHL₁₇₂ in cells may provide a growth advantage to affect the tumor progression and the physiological impact of the balance of expression of pVHL₂₁₃ and/or pVHL₁₇₂ remain to be explored.

MATERIALS AND METHODS

Plasmids

The plasmids pcDNA3.1-*P*_{PGK}-FlagHA-VHL₂₁₃ and -VHL₁₇₂ were generated as follows. The ORF of VHL variant 1 (excised from pCMV2c-VHL₂₁₃, a generous gift from Dr A. Buchberger, Würzburg, Germany) or variant 2 (AA 2-172; GenBank NM_198156) was subcloned in pcDNA3.1-FlagHA (a kind gift from Dr S. Rouquier, Toulouse, France) with murine phosphoglycerate kinase (PGK) promoter. Sanger sequencing confirmed all construct sequences.

Cell culture and transfections

The 786-O kidney cancer cell line, from the ATCC (LGC Standards), was cultured in RPMI-1640 (Gibco™ - Life Technologies) supplemented with 10% fetal calf serum and 1% penicillin/streptomycin at 37°C with 5% CO₂. Stable cell lines were generated by transfecting 786-O cells with pcDNA3.1-*P*_{PGK}-Flag-HA-VHL₂₁₃ or pcDNA3.1-*P*_{PGK}-Flag-HA-VHL₁₇₂ using JetPRIME (PolyPlus, Ozyme) and selected with 500µg/ml G418 (Gibco™). *VHL* knockdown experiments were performed by transfecting 75 nM siRNA against *VHL* variant 2 or a control siRNA [3] using JetPRIME for 72 hours. Cells were then harvested for western blotting and RT-PCR analysis.

RNA extraction and RT-qPCR analysis

Total RNA was extracted from cells using the Nucleospin RNA reagent kit (Macherey-Nagel). cDNAs were synthesized from 1.5 µg (or 0.4 µg from spheroids) total RNA using random hexamer primers and M-MLV reverse transcriptase (Promega). All primers used for quantitative PCR (qPCR) are summarized in Supplementary Tables 2 and 3. PCR reactions were carried out using the GoTaq Flexi DNA Polymerase kit (Promega) and qPCR was performed as previously described [43].

Protein extraction and immunoblotting

Cells were lysed in extraction buffer (EB) or in RIPA buffer [3], or directly in SDS-PAGE loading buffer. Equal amounts of proteins were separated by SDS-PAGE. Membranes were probed with antibodies against VHL (1:1,000; clone JD1956), HA (1:4,000; Roche), Flag (1:2,000; Sigma-Aldrich), β-tubulin (1:2,000; Sigma-Aldrich), cyclin D1 (1:500; Cell Signaling Technology), cullin-2 (1:450; Invitrogen™, Life Technologies), elongin-C (1:1,000; Bio Legend), HIF2-α (1:500; Novus Biologicals). Immune complexes were detected as described [3].

Immunoprecipitation assays

Total protein extracts (250 µg/sample) in EB buffer were incubated with anti-Flag antibody (Sigma-Aldrich). Then 15µl of Affi-Prep® Protein A (Bio-Rad) were incubated with the mixture. Bound fractions were solubilized in SDS-PAGE loading buffer and analysed as described in [3].

Zymography assay

Twenty µg of total protein extracts were separated in denaturing and non-reducing conditions on 8% polyacrylamide gels containing 1mg/ml gelatin type B (Sigma) or 0.5 mg/ml collagen type I (Sigma). Gels were washed twice with 2.5% Triton® X-100 for 20 min to eliminate SDS. After washes in buffer (50mM Tris pH8.0, 150mM NaCl, 5mM CaCl₂, 2µM ZnCl₂), gels were incubated in activation buffer at 37°C for 16 hours, and then stained with Coomassie® Blue.

Immunofluorescence

Cells were cultured on coverslips for 48 hours and fixed with 3.7% paraformaldehyde. Cells were processed for immunocytochemistry as previously described [44] and stained with the rat anti-HA antibody (1/50 in PBS -1% BSA; Roche), followed by the secondary Alexa Fluor®647-conjugated anti-rat secondary antibody (1:1000; Abcam). Images were analysed with the ImageJ software (NIH).

Immunohistochemistry

Four-µm sections of formalin-fixed, paraffin-embedded tumor samples were processed for immunohistochemistry, as previously described [16]. The anti-HA antibody (1:200; Roche) binding was revealed with horseradish peroxidase (HRP)-labelled polymer conjugated to secondary antibodies (Envision™ + Dual Link System-HRP, DAKO) and diaminobenzidine as chromogen (Sigma-Aldrich). CD31 immunostaining (1:25; Clinisciences) was performed using an automated slide staining system (Discovery XT -Ventana Medical Systems). Whole slide image acquisition was performed using a Nanozoomer 2.0-HT and the NDP.view2 viewing software (Hamamatsu).

Proliferation assay

Cells were seeded in 96-well plates (500 cells/well) and cell proliferation was analyzed after 0, 2, 3, 4 or 5 days of culture. The PrestoBlue™ reagent (Invitrogen) was added according to the manufacturer's recommendation and fluorescence was quantified using a microplate reader (FLUOstar Omega – BMG Labtech).

Wound healing assay

Cells were cultured at 5% CO₂ at 37°C until confluence and then a scratch was performed manually. Cells were treated or not with 10µg/ml mitomycin C (Sigma-Aldrich). Cell migration was then recorded every hour for 24 hours using an Axiovert 200M microscope equipped with a LD Plan-Neofluar 20×/0.4 Ph2 lens and an AxioCam MRm camera under the control of the ZEN 2012 software (Zeiss). The wound area was measured using the SimplePCI6 software (Hamamatsu).

Spheroid formation

5,000 cells were plated in medium in a well of a 96-well plate with round bottom previously coated with Poly(2-hydroxyethyl metacrylate) (Sigma) and incubated for 4 days to allow spheroid formation. The spheroids were analysed by microscopy (DMIRB- Leica) and the size calculated using Image J software.

In vivo xenograft experiments

Five-week-old nude mice (BALB/cAnNRj-Foxn1nu/Foxn1nu; Janvier Laboratories) were subcutaneously injected with 786-O-pVHL₁₇₂ cells on the left flank and with 786-O or 786-O-pVHL₂₁₃ cells on the right flank (1.10⁷ cells/injection; five animals/group). Tumor size was monitored using an electronic calliper twice per week. Tumor volume was determined according to the equation: Vol. = length x width x thickness x 0.5236. Mice were finally euthanized and tumors harvested and cut in two pieces (one snap-frozen and the other formalin-fixed). The experimental protocol complied with the institution's guidelines for animal welfare and was approved by the Ethics Committee for Animal Experimentation of the French Ministry for Higher Education and Scientific Research (agreement # 2015072410433840 v2).

Statistical analyses

Statistical analyses were performed with the R-studio software. Statistical significance was assessed using unpaired Student t, Kruskal-Wallis, Mann-Whitney and ANOVA tests. P < 0.05 was considered significant.

ACKNOWLEDGMENTS

We would like to acknowledge S. Dreano (IGDR) for his contribution in plasmids sequencing. We acknowledge P. Bellaud, R. Viel and M. Seffals from the High Precision Histo Pathology (H2P2) facility at the BIOSIT for their expertise in immunohistochemistry. We would like to thank the ImpACell and MRic microscopy

platforms for fluorescence microscopy-equipment and ARCHE (animal housing facility) at the SFR BIOSIT CNRS UMS3480 Rennes.

CONFLICTS OF INTEREST

The authors declare no conflicts of interest.

FUNDING

The authors would like to acknowledge funding attributed to this study, research grants from “La Ligue contre le cancer 2015-2016” and the financial support from the French ARC (Association pour la Recherche sur le Cancer) for P. Hascoet.

REFERENCES

1. Blankenship C, Naglich JG, Whaley JM, Seizinger B, Kley N. Alternate choice of initiation codon produces a biologically active product of the von Hippel Lindau gene with tumor suppressor activity. *Oncogene*. 1999; 18:1529–35.
2. Schoenfeld A, Davidowitz EJ, Burk RD. A second major native von Hippel-Lindau gene product, initiated from an internal translation start site, functions as a tumor suppressor. *Proc Natl Acad Sci USA*. 1998; 95:8817–22.
3. Chesnel F, Hascoet P, Gagné JP, Couturier A, Jouan F, Poirier GG, Le Goff C, Vigneau C, Danger Y, Verite F, Le Goff X, Arlot-Bonnemains Y. The von Hippel-Lindau tumour suppressor gene: uncovering the expression of the pVHL172 isoform. *Br J Cancer*. 2015; 113:336–44.
4. Gnarr JR, Tory K, Weng Y, Schmidt L, Wei MH, Li H, Latif F, Liu S, Chen F, Duh FM, Lubensky I, Duan DR, Florence C, et al. Mutations of the VHL tumour suppressor gene in renal carcinoma. *Nat Genet*. 1994; 7:85–90.
5. Iliopoulos O, Kibel A, Gray S, Kaelin WG Jr. Tumour suppression by the human von Hippel-Lindau gene product. *Nat Med*. 1995; 1:822–26.
6. Mao S, Huang S. The signaling pathway of hypoxia inducible factor and its role in renal diseases. *J Recept Signal Transduct Res*. 2013; 33:344–48.
7. Banks RE, Tirukonda P, Taylor C, Hornigold N, Astuti D, Cohen D, Maher ER, Stanley AJ, Harnden P, Joyce A, Knowles M, Selby PJ. Genetic and epigenetic analysis of von Hippel-Lindau (VHL) gene alterations and relationship with clinical variables in sporadic renal cancer. *Cancer Res*. 2006; 66:2000–11.
8. Esteban-Barragán MA, Avila P, Alvarez-Tejado M, Gutiérrez MD, García-Pardo A, Sánchez-Madrid F, Landázuri MO. Role of the von Hippel-Lindau tumor suppressor gene in the formation of beta1-integrin fibrillar adhesions. *Cancer Res*. 2002; 62:2929–36.

9. Li M, Kim WY. Two sides to every story: the HIF-dependent and HIF-independent functions of pVHL. *J Cell Mol Med.* 2011; 15:187–95.
10. Ananth S, Knebelmann B, Grüning W, Dhanabal M, Walz G, Stillman IE, Sukhatme VP. Transforming growth factor beta1 is a target for the von Hippel-Lindau tumor suppressor and a critical growth factor for clear cell renal carcinoma. *Cancer Res.* 1999; 59:2210–16.
11. Boström AK, Lindgren D, Johansson ME, Axelson H. Effects of TGF- β signaling in clear cell renal cell carcinoma cells. *Biochem Biophys Res Commun.* 2013; 435:126–33.
12. Moustakas A, Heldin CH. The regulation of TGFbeta signal transduction. *Development.* 2009; 136:3699–714.
13. Martella M, Salviati L, Casarin A, Trevisson E, Opocher G, Polli R, Gross D, Murgia A. Molecular analysis of two uncharacterized sequence variants of the VHL gene. *J Hum Genet.* 2006; 51:964–68.
14. Taylor C, Craven RA, Harnden P, Selby PJ, Banks RE. Determination of the consequences of VHL mutations on VHL transcripts in renal cell carcinoma. *Int J Oncol.* 2012; 41:1229–40.
15. Schwanhäusser B, Busse D, Li N, Dittmar G, Schuchhardt J, Wolf J, Chen W, Selbach M. Global quantification of mammalian gene expression control. *Nature.* 2011; 473:337–42.
16. Ghajar CM, George SC, Putnam AJ. Matrix metalloproteinase control of capillary morphogenesis. *Crit Rev Eukaryot Gene Expr.* 2008; 18:251–78.
17. Krishnamachary B, Berg-Dixon S, Kelly B, Agani F, Feldser D, Ferreira G, Iyer N, LaRusch J, Pak B, Taghavi P, Semenza GL. Regulation of colon carcinoma cell invasion by hypoxia-inducible factor 1. *Cancer Res.* 2003; 63:1138–43.
18. Muñoz-Nájjar UM, Neurath KM, Vumbaca F, Claffey KP. Hypoxia stimulates breast carcinoma cell invasion through MT1-MMP and MMP-2 activation. *Oncogene.* 2006; 25:2379–92.
19. Yang S, Kim J, Ryu JH, Oh H, Chun CH, Kim BJ, Min BH, Chun JS. Hypoxia-inducible factor-2alpha is a catabolic regulator of osteoarthritic cartilage destruction. *Nat Med.* 2010; 16:687–93.
20. Tanimoto K, Makino Y, Pereira T, Poellinger L. Mechanism of regulation of the hypoxia-inducible factor-1 alpha by the von Hippel-Lindau tumor suppressor protein. *EMBO J.* 2000; 19:4298–309.
21. Kominsky SL, Doucet M, Thorpe M, Weber KL. MMP-13 is over-expressed in renal cell carcinoma bone metastasis and is induced by TGF-beta1. *Clin Exp Metastasis.* 2008; 25:865–70.
22. Maxwell PH, Wiesener MS, Chang GW, Clifford SC, Vaux EC, Cockman ME, Wykoff CC, Pugh CW, Maher ER, Ratcliffe PJ. The tumour suppressor protein VHL targets hypoxia-inducible factors for oxygen-dependent proteolysis. *Nature.* 1999; 399:271–75.
23. Hsu T, Adereth Y, Kose N, Dammai V. Endocytic function of von Hippel-Lindau tumor suppressor protein regulates surface localization of fibroblast growth factor receptor 1 and cell motility. *J Biol Chem.* 2006; 281:12069–80.
24. Benjamin LE, Golijanin D, Itin A, Pode D, Keshet E. Selective ablation of immature blood vessels in established human tumors follows vascular endothelial growth factor withdrawal. *J Clin Invest.* 1999; 103:159–65.
25. Edeline J, Mottier S, Vigneau C, Jouan F, Perrin C, Zerrouki S, Fergelot P, Patard JJ, Rioux-Leclercq N. Description of 2 angiogenic phenotypes in clear cell renal cell carcinoma. *Hum Pathol.* 2012; 43:1982–90.
26. Cheville JC, Lohse CM, Zincke H, Weaver AL, Leibovich BC, Frank I, Blute ML. Sarcomatoid renal cell carcinoma: an examination of underlying histologic subtype and an analysis of associations with patient outcome. *Am J Surg Pathol.* 2004; 28:435–41.
27. Izquierdo E, Cañete JD, Celis R, Santiago B, Usategui A, Sanmartí R, Del Rey MJ, Pablos JL. Immature blood vessels in rheumatoid synovium are selectively depleted in response to anti-TNF therapy. *PLoS One.* 2009; 4:e8131.
28. Barry RE, Krek W. The von Hippel-Lindau tumour suppressor: a multi-faceted inhibitor of tumourigenesis. *Trends Mol Med.* 2004; 10:466–72.
29. Cheville JC, Frank I, Leibovich BC, Lohse CM, Blute ML. Re: Renal vein or inferior vena caval extension in patients with renal cortical tumors: impact of tumor histology. *J Urol.* 2004; 172:1196.
30. Cates JM, Dupont WD, Barnes JW, Edmunds HS, Fasig JH, Olson SJ, Black CC. Markers of epithelial-mesenchymal transition and epithelial differentiation in sarcomatoid carcinoma: utility in the differential diagnosis with sarcoma. *Appl Immunohistochem Mol Morphol.* 2008; 16:251–62.
31. Wendt MK, Allington TM, Schiemann WP. Mechanisms of the epithelial-mesenchymal transition by TGF-beta. *Future Oncol.* 2009; 5:1145–68.
32. Lebdai S, Verhoest G, Parikh H, Jacquet SF, Bensalah K, Chautard D, Rioux Leclercq N, Azzouzi AR, Bigot P. Identification and validation of TGFBI as a promising prognosis marker of clear cell renal cell carcinoma. *Urol Oncol.* 2015; 33:69.e11-8. <https://doi.org/10.1016/j.urolonc.2014.06.005>.
33. Shang D, Liu Y, Yang P, Chen Y, Tian Y. TGFBI-promoted adhesion, migration and invasion of human renal cell carcinoma depends on inactivation of von Hippel-Lindau tumor suppressor. *Urology* 2012; 79: 966 e961-967.
34. Selvamurugan N, Kwok S, Partridge NC. Smad3 interacts with JunB and Cbfa1/Runx2 for transforming growth factor-beta1-stimulated collagenase-3 expression in human breast cancer cells. *J Biol Chem.* 2004; 279:27764–73.
35. Kallakury BV, Karikhalli S, Haholu A, Sheehan CE, Azumi N, Ross JS. Increased expression of matrix metalloproteinases 2 and 9 and tissue inhibitors of metalloproteinases 1 and 2 correlate with poor prognostic

- variables in renal cell carcinoma. *Clin Cancer Res.* 2001; 7:3113–19.
36. Kitagawa Y, Kunimi K, Uchibayashi T, Sato H, Namiki M. Expression of messenger RNAs for membrane-type 1, 2, and 3 matrix metalloproteinases in human renal cell carcinomas. *J Urol.* 1999; 162:905–09.
 37. Bauvois B. New facets of matrix metalloproteinases MMP-2 and MMP-9 as cell surface transducers: outside-in signaling and relationship to tumor progression. *Biochim Biophys Acta* 2012; 1825: 29-36.
 38. Sassano A, Mavrommatis E, Arslan AD, Kroczyńska B, Beauchamp EM, Khuon S, Chew TL, Green KJ, Munshi HG, Verma AK, Plataniias LC. Human Schlafen 5 (SLFN5) Is a Regulator of Motility and Invasiveness of Renal Cell Carcinoma Cells. *Mol Cell Biol.* 2015; 35:2684–98.
 39. Johansson N, Ala-aho R, Uitto V, Grénman R, Fusenig NE, López-Otín C, Kähäri VM. Expression of collagenase-3 (MMP-13) and collagenase-1 (MMP-1) by transformed keratinocytes is dependent on the activity of p38 mitogen-activated protein kinase. *J Cell Sci.* 2000; 113:227–35.
 40. Essers PB, Klasson TD, Pereboom TC, Mans DA, Nicastro M, Boldt K, Giles RH, MacInnes AW. The von Hippel-Lindau tumor suppressor regulates programmed cell death 5-mediated degradation of Mdm2. *Oncogene.* 2015; 34:771–79.
 41. Lawson KA, Teteak CJ, Yang L, Gee AO, Chansky HA, Garrity JT, Stoker AM, Cook JL. Analyzing chondrocyte viability: letter to the editor. *Am J Sports Med.* 2013; 41:NP29–30.
 42. Cai Z, Wang Y, Yu W, Xiao J, Li Y, Liu L, Zhu C, Tan K, Deng Y, Yuan W, Liu M, Wu X. hnulp1, a basic helix-loop-helix protein with a novel transcriptional repressive domain, inhibits transcriptional activity of serum response factor. *Biochem Biophys Res Commun.* 2006; 343:973–81.
 43. Charlier C, Montfort J, Chabrol O, Brisard D, Nguyen T, Le Cam A, Richard-Parpaillon L, Moreews F, Pontarotti P, Uzbekova S, Chesnel F, Bobe J. Oocyte-somatic cells interactions, lessons from evolution. *BMC Genomics.* 2012; 13:560.
 44. Dugay F, Le Goff X, Rioux-Leclercq N, Chesnel F, Jouan F, Henry C, Cabillic F, Verhoest G, Vigneau C, Arlot-Bonnemains Y, Belaud-Rotureau MA. Overexpression of the polarity protein PAR-3 in clear cell renal cell carcinoma is associated with poor prognosis. *Int J Cancer.* 2014; 134:2051–60.